American Mineralogist, Volume 89, pages 473–484, 2004

A zero-damage model for fission-track annealing in zircon

MEINERT K. RAHN,[1,*] MARK T. BRANDON,[2] GEOFFREY E. BATT,[3] AND JOHN I. GARVER[4]

[1]Institut für Mineralogie, Petrologie und Geochemie, Albert-Ludwigs-Universität, Freiburg, Germany
[2]Department of Geology and Geophysics, Yale University, New Haven, Connecticut, 06520-8109 U.S.A.
[3]Department of Geology, Royal Holloway University of London, Egham, Surrey, U.K.
[4]Geology Department, Union College, Schenectady, New York, 12308 U.S.A.

ABSTRACT

A zircon fission track-annealing model is calculated on the basis of annealing experiments from the literature with induced tracks in α-decay event damage-free zircon samples. Empirically derived parallel and fanning equations for this "zero-damage" model yield an excellent fit to the data, with the fanning model providing slightly better statistical parameters. A comparison between annealing models with fanning iso-annealing lines but different α-decay event damage densities reveals that annealing temperatures and closure temperatures for the estimated partial annealing zone are highest for the zero-damage model.

Compilations of existing geologic constraints on the zircon partial-annealing zone on one hand and the zircon closure temperature on the other show that these constraints do not or only partly overlap with curves of proposed models for the zircon partial-annealing zone and closure temperature. This finding is consistent with the fact that the annealing behavior of zircon from long-duration temperature evolutions is increasingly influenced by the accumulated α-decay event damage. Zircon samples of young age or low U content show a behavior closest to the predictions of the zero-damage model, and are in the predicted range of published models with low α-decay event damage density. For thermal events of more than 10 myr duration, however, constraints from field studies show marked differences from proposed partial-annealing zone boundaries of the zero- or low-damage models.

The applicability of the zero-damage model is threefold. (1) It predicts correct closure temperatures in the case of very rapid cooling across the partial annealing zone where basically no α-decay event damage is accumulated. (2) It predicts an uppermost boundary for complete annealing of a mixture of zircon components of different age, as found in sedimentary samples, and in this case may be used as a thermometer. (3) It represents an important reference for the establishment of a more comprehensive model of zircon fission-track annealing that also includes the influence of α-decay event damage. For such a model, two different equations are discussed. However, additional detailed experimental and field data are needed for a more robust annealing model that includes the influence of α-decay event-damage annealing.

INTRODUCTION

Zircon is a common accessory mineral in magmatic rocks of intermediate to felsic composition and their metamorphic and sedimentary counterparts. It is one of the most important storage minerals for U and Th, and has therefore been among the first and most extensively used minerals in dating of rocks of different origin. Zircon has been dated by the U-Pb method since the early 1950s (Larsen et al. 1952), and was one of the first minerals to be dated with the fission-track (FT) method (Fleischer et al. 1964). Because annealing of FTs in zircon commonly takes place at sub-greenschist facies conditions on a geologic time scale, this dating method has mainly been used to study late-stage cooling, together with other chronometers (e.g., Zeitler 1985; Hurford 1986), or near-surface thermal histories (e.g., Hasebe et al. 1997, 2003). To accomplish this goal, zircon samples have been sampled at or below the surface in order to gain an on-site exhumation history. Alternatively, zircon FT ages from sedimentary rocks have been used in conjunction with the sedimentary age to restore the exhumation history of the provenance area, and to unravel erosion and transport patterns (e.g. Garver and Brandon 1994; Garver et al. 1999). For such an application, it is imperative to understand the thermal behavior and stability of tracks in zircon in order to interpret the thermal significance of the measured FT age and track-length distribution.

Similar to apatite (see e.g., Laslett et al. 1987; Gallagher 1995; Willett 1997; Ketcham et al. 1999), zircon FT ages and track-length distributions have the potential to predict cooling paths. However, zircon annealing models for time-temperature modeling have not yet found the wide application as those models for apatite, in particular due to the lack of knowledge on the influence of composition and accumulated radiation damage to its annealing behavior.

Fleischer et al. (1965) published the first data on zircon FT annealing, using experiments with natural fission tracks, but only three states were distinguished: total track removal, partly faded tracks, and unaltered tracks. Their proposed linear bound-

*Present address: Swiss Federal Nuclear Safety Inspectorate, 5232 Villigen-HSK, Switzerland. E-mail: rahn@hsk.ch

ary passes between experimental runs with unaltered tracks on one side and runs with partly faded tracks on the other, and thus represents a lower boundary (with respect to temperature) of the partial annealing zone (PAZ), a transitional temperature zone between complete conservation and complete annealing of FTs. Extrapolated to geologic time scales, their prediction for the lower PAZ boundary for a 1 myr annealing time was above 350 °C (Fig. 1a, the term "myr" refers to a time duration in this study, while "Ma" is used for a specific moment in time). Krishnaswami et al. (1974) used a similar classification for their experimental results, and estimated a lower PAZ boundary at 310 °C for a 1 myr annealing duration. Both results seemed at odds with geologic field studies, as the zircon FT ages were systematically younger than K-Ar data on muscovite or biotite for which closure temperatures of 300 and 350 °C, respectively, were estimated under geologic conditions (e.g., Harrison et al. 1979; Hurford 1986).

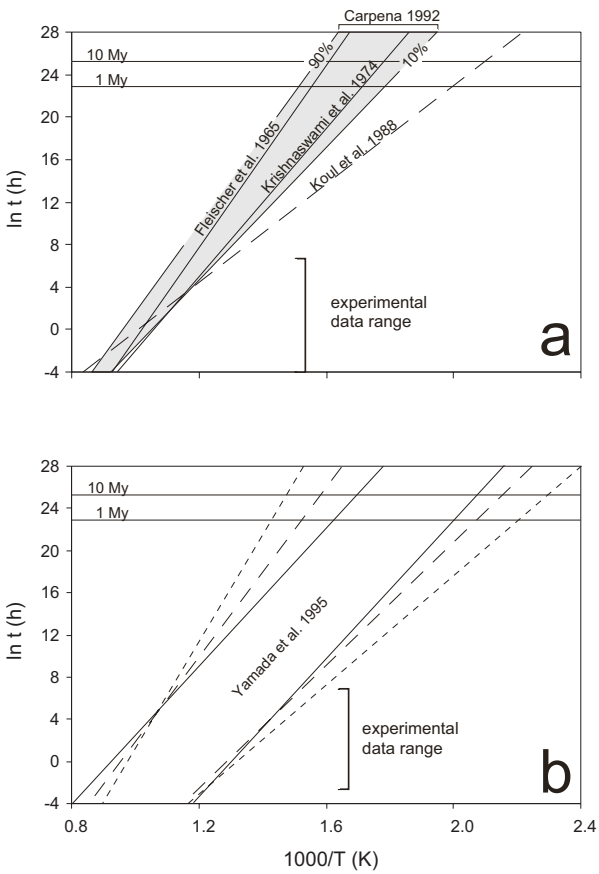

FIGURE 1. Compilation of published zircon FT PAZ boundaries in an Arrhenius plot. **(a)** PAZ boundaries of Fleischer et al. (1965), Krishnaswami et al. (1974), Koul et al. (1988), and Carpéna (1992) (shaded area). The lines of Fleischer et al. (1965) and Krishnaswami et al. (1974) were considered to be the low-*T* side of the PAZ. The Koul et al. (1988) line was proposed as an upper PAZ boundary. For the PAZ boundaries of Carpéna (1992), lines of 10 and 90% of track density reduction are shown. **(b)** PAZ boundaries of the three proposed models of Yamada et al. (1995): solid line = parallel model; long-dashed line = fanning model with $T_0 \neq \infty$; short-dashed line = fanning model with $T_0 = \infty$. All boundaries are directly taken from Yamada et al. (1995), and correspond to track length ratios (L/L_0) of 0.95 and 0.4 and track-density ratios (ρ/ρ_o) of 0.94 and 0.25. Note the large differences of the models when extrapolated to geologic time scales.

Two studies on induced track lengths were published by Koul et al. (1988) and Carpéna (1992), but differ strongly from each other (Fig. 1a). Zircon samples with induced tracks were produced by total annealing of the natural tracks, and then inducing tracks with thermal neutrons in a reactor facility. Although Koul et al. (1988) only reported their curve for total annealing (corresponding to an upper PAZ boundary), Carpéna (1992) listed all experimental runs and estimated contours for track-density reduction. Figure 1a shows Carpéna's 10 and 90% contours, which were adopted to define the zircon PAZ. This estimated PAZ overlaps with the curves of Fleischer et al. (1965) and Krishnaswami et al. (1974).

More recently, Yamada et al. (1995) presented an experimental data set that was suitable to define and test different annealing models (Fig. 1b). These authors, as well as Galbraith and Laslett (1997) who published a more-refined statistical treatment on the data set, considered two empirical fit equations: one corresponding to an equation with parallel lines and another to an equation with fanning iso-annealing lines in an Arrhenius plot. Both groups agreed that the data do not clearly favor one equation over the other. Two new long-term annealing data were added by Tagami et al. (1998), and the enlarged data set fitted according to the statistical procedure of Galbraith and Laslett (1997). In those data sets, the relationship with fanning iso-annealing lines commonly provides a better fit to the data. Figure 1b illustrates three proposed relationships: one with parallel lines, called hereafter "parallel relationship" or "parallel equation," and two with fanning iso-annealing lines, called "fanning equations" (Yamada et al. 1995). The results of these equations markedly differ from each other when extrapolated to geologic time scales.

Direct comparison between experimental annealing data from different studies is complicated by the following problems. (1) Sample treatment, in particular etching, is a major source of variation for FT lengths in zircon (Amin 1988; Tagami et al. 1990; Hasebe et al. 1993), and may account for differences among experiments that otherwise included the same *t-T* conditions. (2) Some studies report track densities, whereas others track lengths. (3) Some annealing studies are based on annealed zircon samples with induced tracks; others used natural zircon samples with varying degrees of α-decay event damage. (4) A problem particular to older studies is that the zircon samples were not sufficiently characterized with respect to age and track density. (5) Finally, there is no generally accepted definition for the zircon PAZ with respect to track density or length reduction.

In contrast to apatite (e.g., Carlson et al. 1999), zircon composition does not appear to be an important factor controlling FT annealing, but this issue needs to be studied in more detail. The influence of α-decay event damage on the annealing of FTs, on the other hand, has received much more attention. The damage produced by α-decay events (hereafter for simplicity called "α damage") is mainly the result of ^{238}U (and to a minor extent of ^{232}Th and ^{235}U) decaying in a multistep process to Pb and causing structural damage that affects the bulk physical properties (see e.g., Murakami et al. 1991; Ewing 1994). Such structural changes

include mainly the damage produced by the recoil nucleus and to a much lesser extent by the expelled α particle (Weber et al. 1994). A single α-recoil track is approximately 25 nm long (depending on the single recoil energy, Palenik et al. 2003), whereas entire decay chains (6–8 decays) produce amorphous domains of up to 100 nm in diameter (Murakami et al. 1991) that, with increasing damage density, start to form percolating clusters (Salje et al. 1999) and eventually lead to complete metamictization. The α particle tracks in zircon measure 13 μm in length (Nasdala et al. 1999), which is similar to the length of etched FTs (Tagami et al 1990). With respect to size, α-recoil tracks are much shorter than FTs, but by comparison of the α and fission decay constants of ^{238}U, ^{235}U, and ^{232}Th, it is evident that the α-decay process is more than 10^7 times more frequent than the fission decay event for ^{238}U, and that this ratio is several orders of magnitude larger for ^{235}U and ^{232}Th due to the very low fission decay constants of ^{235}U and ^{232}Th. The status of damage accumulation in zircon is determined by changes in measured macroscopic (e.g., Holland and Gottfried 1955) as well as microscopic patterns (e.g., Nasdala et al. 1995; Ríos et al. 2000; Farnan and Salje 2001; Zhang et al. 2001) and show that the crystalline-to-amorphous transition is characterized by two distinct transitions (Salje et al. 1999), and that the amorphous phase shows polymerization (Farnan and Salje 2001) as well as density differences on the atomic scale (Trachenko et al. 2003).

In a study of four different zircon samples with natural FT densities between 0.87 and $9.95 \cdot 10^6$/cm^2 and their annealed counterparts with induced tracks, Kasuya and Naeser (1988) were able to demonstrate that α-damage-free zircon samples are systematically more retentive of fission tracks relative to their natural counterparts. Because of the approximately constant ratio of α-decay events to fission decays, annealing behavior might be expected to correlate with spontaneous track density, but their experiments did not show any obvious correlation. A similar behavior of track stability as a function of α damage was observed by Yamada et al. (1995).

The annealing of etchable FTs in zircon was shown to occur at 400–800 °C in short-term laboratory experiments (Carpéna 1992; Yamada et al. 1995; Tagami et al. 1998) and at 200–350 °C for geologic time spans (Tagami and Shimada 1996; Tagami et al. 1995a; Brandon et al. 1998; Hasebe et al. 2003). In contrast, for the annealing of α damage in zircon under laboratory and geologic conditions, a variety of observations gives a very complex picture: Garver and Kamp (2002) showed that zircon color, which is a result of point defects in crystalline areas, is annealed during geologic time scales at reasonably low temperatures of 350–400 °C, i.e., at conditions above the FT PAZ. Short-term laboratory heating of a partially metamict zircon to temperatures up to about 700 °C only induced the removal of defects within the crystalline remnants, whereas epitaxial recrystallization of the amorphous part needed temperatures in excess of 700 °C (e.g., Chakoumakos et al. 1987; Zhang et al. 2000; Capitani et al. 2000; Geisler 2002). Total recovery of the crystal structure was achieved only at temperatures of 1400 to 1600 °C, with the observed decomposition into ZrO_2 and SiO_2 in heavily metamict zircon samples (Capitani et al. 2000). On this basis it has to be assumed that a strong reduction in damage only takes place at temperatures in excess of those need for FT annealing.

Because FT annealing in zircon is influenced by the amount of accumulated α damage (Kasuya and Naeser 1988; Yamada et al. 1995), the relationship between α damage and FT annealing has major implications for the interpretation of FT data. Under geologic conditions, when zircon samples enter the PAZ from the high-temperature side at slow to moderate cooling rates, they will accumulate significant amounts of α damage before the first retention of fission tracks. Fast cooling zircon samples, however, will only experience little α damage accumulation before the entrance into the FT PAZ. As a consequence, they will not have the same annealing properties, but FT retention in cooling zircon samples will be influenced by the individual cooling rate and the U content of each zircon grain. For very fast cooling rates, the FT retention may approach a behavior with no α-damage influence and thus may be predicted by experiments on α-damage-free zircon samples with induced tracks. Zircon samples entering the FT PAZ at its lower boundary will have an annealing behavior in accordance with their residence time below the PAZ (corresponding to the time of α-damage accumulation) and their U content.

In the present study, we present a review of all published FT annealing data on zero-damage zircon samples, develop a procedure for comparing them across differences among the data sets and the chosen experimental approaches, and calculate a zero-damage annealing model. The term "zero-damage" refers to experiments on zircon samples where a total annealing of the radiation damage was achieved by heating of the zircon samples to temperatures of 800 °C or above. These zircon samples are assumed to contain no radiation damage, as opposed to young natural zircon samples (e.g., Yamada et al. 1995), which here are referenced as "low-damage" zircon samples. With the help of the zero-damage model, we will be able to (1) explain several field observations in various geologic settings that could not be explained by previous models and (2) develop the basis for a future model that integrates α damage as a third component affecting zircon FT annealing apart from temperature and time.

FT ANNEALING IN ZERO-DAMAGE ZIRCON

Three sets of induced FT annealing data exist that supply sufficient information about the experimental conditions and the samples used (Kasuya and Naeser 1988; Carpéna 1992; Yamada et al. 1995). Kasuya and Naeser (1988) presented data on four different zircon samples annealed over a temperature range of 400 to 675 °C, but their study only included experiments of 1 h duration. Another 1 h data set is provided by Yamada et al. (1995). The only study that extends to heating times other than 1 h is that of Carpéna (1992) on a totally annealed Mont Blanc zircon sample. Not used for our model are data on induced FT annealing in zircon by Koul et al. (1988), because their study did not provide any annealing data apart from a line of total annealing (Fig. 1a, their Fig. 7), and by Koshimizu (1993), because his observations on differences between internal (4π) and external (2π) surfaces have raised the question of a methodical problem within this study. In the three remaining experimental studies, annealing in zircon was studied by step heating of zircon aliquots for time periods from 5 min to 917 h and constant temperatures between 397 and 800 °C.

A comparison of all 1 h experiments reveals that these data

lie close to a common curve on a L/L_0 vs. annealing temperature diagram (L = measured mean track length, L_0 = measured initial mean track length before annealing), despite the fact that the data originate from three different labs, and etching conditions were very different (Fig. 2a). For comparison, three sets of annealing experiments at 1 h from zircon samples of different age (Tagami et al. 1990; Yamada et al. 1995) show distinct differences in annealing behavior and a clear trend of decreasing track stability with increasing age, and therefore accumulated α damage (Fig. 2b), although part of the differences may be explained by differences in etching conditions (T. Tagami, personal communication). The original data of Carpéna (1992), given as track density ratios ρ/ρ_0, have been converted to L/L_0 using a relationship from Tagami et al. (1990). The use of the L/L_0 ratio instead of absolute measured lengths provides a way of avoiding differences among labs in observed maximum length. For instance, for induced tracks, Kasuya and Naeser (1988) reported a mean L_0 = 10.84 (no error given[1]) µm, whereas Yamada et al. (1995) reported L_0 = 11.03 (±0.10, 1 SE) µm.

In our analysis, we used the set of measured track lengths for zero-damage zircon data from Yamada et al. (1995). Their distinction between the means of all track lengths (L_{all}) and those with an angle >60° to the *c*-axis ($L_{>60}$) is avoided for several reasons. First, the plotting of their L_{all} and $L_{>60}$ values reveals that the resulting correlation is significantly different from a 1:1 relationship (Fig. 3), but many single values and their standard deviation are not. Second, the restricted data set ($L_{>60}$) has distinctly smaller track-length numbers, which leads to poorer statistics for young and U-poor zircon samples. Third, from a practical point of view, the distinction between L_{all} and $L_{>60}$ is difficult to apply to samples with sub- and anhedral zircon grains and very low track densities. Finally, similar to the behavior observed with apatite track lengths (see Ketcham et al. 1999), the relationship between the reduction of track length and the track angle to the *c*-axis may be more complicated in zircon, requiring more detailed investigations. We therefore prefer to use a measure that is representative of the way that FTs in zircon samples are currently measured. Carpéna (1992) observed different annealing rates as a function of zircon topology (sensu Pupin 1980). This distinction is again difficult to apply to non-euhedral zircon samples. Instead, we seek to characterize the annealing properties of all zircon samples so that the results will be more relevant for current practices in zircon FT dating.

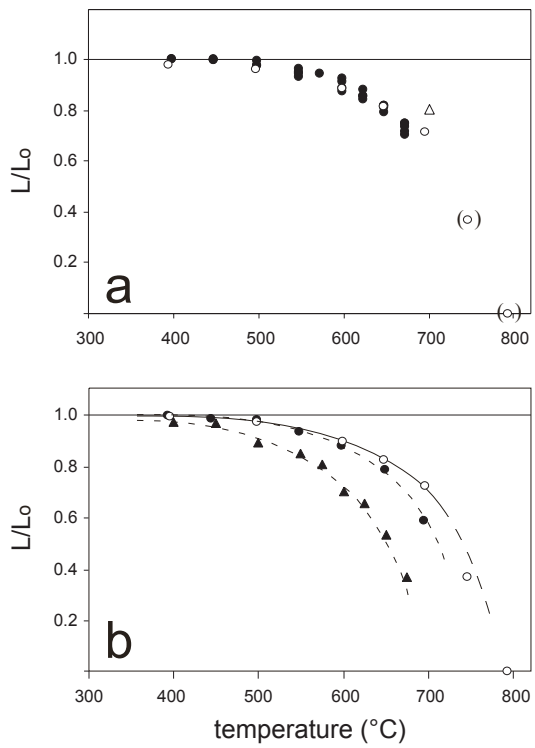

FIGURE 2. Comparison of 1 hour FT annealing experiments for zircon samples in normalized track length vs. temperature diagrams: (**a**) annealing experiments on annealed zircon samples with induced tracks. Filled circles = Kasuya and Naeser (1988); open circles = Yamada et al. (1995) = triangle: Carpéna (1992). The two data points in parentheses represent estimated values. (**b**) annealing experiments on zircon samples with different levels of α-damage density. Open circles as in **a**, filled circles = annealing in 21 Ma zircon samples (track density ~4×10^6/cm^2) from Yamada et al. (1995); filled triangles = annealing in 69 Ma zircon samples (track density ~7×10^6/cm^2) from Tagami et al. (1990).

[1] Kasuya and Naeser (1988) reported "no significant difference in the initial track lengths (10.7–10.9 µm)" in their investigated zircon samples. This result suggests a 2σ standard error of the mean (SE) of 0.1 µm.

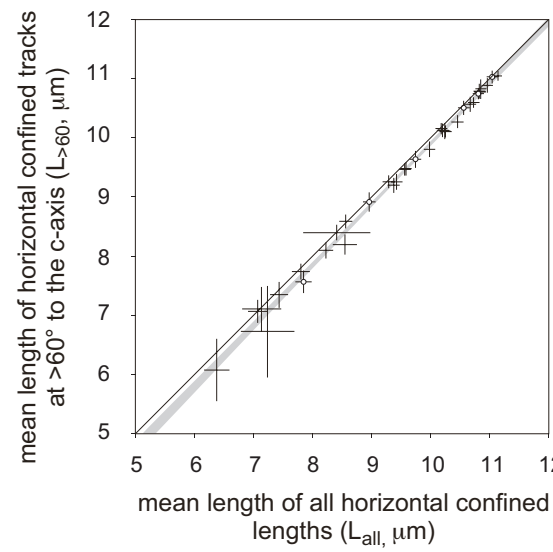

FIGURE 3. Comparison of the mean track lengths for all orientations (L_{all}) with those of tracks at an angle >60° to the crystallographic *c*-axis ($L_{>60}$). Data from Tagami et al. (1998) and Yamada et al. (1995). Error bars shown as 1 SE. Data from zero-damage zircon samples are marked with open circles. The errors of the L_{all} values were estimated according to the empirical relationship in Figure 4. Means for L_{all} and L are indistinguishable from a 1:1 relationship (diagonal line) based on the displayed 68% confidence interval. The grey shaded area represents the 2 SE uncertainty for a linear regression fit for all L_{all} and $L_{>60}$ values ($L_{>60} = 1.029 * L_{all} - 0.381$), which is slightly but significantly different from a 1:1 relationship.

THE ZERO-DAMAGE MODEL

The fanning and parallel models, first developed for apatite FT dating (for a review, see Ketcham et al. 1999), were examined as possible empirical annealing equations for the zircon FT system (Yamada et al. 1995; Galbraith and Laslett 1997; Tagami et al. 1998). The applied procedure is to transform L/L_0 to a new variable γ, where:

$$\gamma = \ln(1 - \frac{L}{L_0}) \tag{1}$$

and to define γ as the dependent variable when estimating parameters for an annealing equation. γ describes the degree of annealing as a function of the independent variables of temperature T (in Kelvin) and time t (in hours). The designation of γ as the dependent variable indicates that measurement errors are largest for that variable and that least-square estimations of parameters can ignore errors in the other two variables T and t. This assumption is supported by the errors given by the different authors who claim that the accuracy in temperature is in the order of ±2 °C, whereas the precision for time is in the range of ±1–2 s. The time precision, however, may in fact be important in short-term experiments due to the time necessary for reaching thermal equilibrium within the zircon grains.

The parallel and fanning models are defined by:

$$\gamma = a_p + b_p\left(\frac{1}{T}\right) + c_p \ln(t) \tag{2}$$

and

$$\gamma = a_f + b_f T \ln(t) + c_f T \tag{3}$$

respectively. Each model has three parameters a, b, and c. In both cases, γ is linear with respect to a, b, and c, and thus can be solved using typical weighted least-squares methods. Equation 2 describes a set of planes in a $\ln(t)$-$(1/T)$-γ space for the parallel model, and Equation 3, a plane set in the $\ln(t)$-T-γ space for the fanning model. For the parallel model, each iso-annealing surface is planar, whereas the fanning model has slightly curved iso-annealing surfaces, as the slope in the $\ln(t)$ direction is temperature dependent. For annealing in apatites, an alternative fanning relationship has been applied (Crowley et al. 1991; Laslett and Galbraith 1996; Ketcham et al. 1999), which allows more flexibility for the fanning point. Galbraith and Laslett (1997) and Tagami et al. (1998) have proposed more complex model equations for zircon samples on the basis of the maximum likelihood method and an internally consistent data set, derived from aliquots of the same material. In view of the heterogeneous provenance of the data set compiled here, which is far from being ideal and was not produced for such a purpose, we restrict ourselves to a simpler data treatment based on the Equations 2 and 3.

From Equation 1 it is evident that when L approaches L_0 (at low temperatures), γ becomes large and its variance will probably be large as well. High-temperature runs, where L approaches 0, will have small γ and low variances, even though some L values might be estimated from only a small number of track-length measurements. This situation is particularly true for the 748 and 795 °C runs of Yamada et al. (1995) where $L = 0$, and for one run at 4.5 minutes and 750 °C that yielded only two measurable track lengths. To account for the non-linear relationship between γ and L, we need to calculate weighting factors for γ to be used in our regression analysis. Galbraith and Laslett (1997) introduced such a weighting treatment for the different single data on zircon, and their method is here adopted.

If the standard error for the mean track length $SE(L)$ is known, the standard error for γ can be estimated by:

$$SE(\gamma) = SE(L)\left|\frac{\partial\gamma}{\partial L}\right| = \left|\frac{SE(L)}{L - L_0}\right| \tag{4}$$

This error estimation ignores errors for L_o given that its uncertainty is small. For annealing experiments reported as track densities, we converted the data to track lengths using the linear relationship of Tagami et al. (1990):

$$\left(\frac{L}{L_0}\right) = a_L + b_L\left(\frac{\rho}{\rho_o}\right) \tag{5}$$

with $a_L = 0.2$ and $b_L = 0.8$. This gives

$$\gamma = \ln\left(1 - a_L - b_L\left(\frac{\rho}{\rho_o}\right)\right) \tag{6}$$

with an uncertainty approximated by

$$SE(\gamma) = SE\left(\frac{\rho}{\rho_o}\right)\left(\frac{-b_L}{1 - a_L - b_L\left(\frac{\rho}{\rho_o}\right)}\right). \tag{7}$$

We used standard weighted regression analysis (e.g., Press et al. 1992) with observations of γ weighted according to:

$$w = \frac{1}{SE(\gamma)^2} \tag{8}$$

Carpéna (1992) reported standard errors for all her density data. Yamada et al. (1995) only give the restricted length measurement set $L_{>60}$. However, because there is a close relationship between $L_{>60}$ and L_{all} (Fig. 3), we use the reported standard deviations from the $L_{>60}$ values, and divide by the square root of the total number of track-length measurements to get standard errors for their L_{all}. Standard errors were not visible for most of the Kasuya and Naeser (1988) data, because the error bars of most data points on their plots are reported to be hidden behind the plotted symbols (the original data were requested, but were no longer available, M. Kasuya, pers. comm.). We therefore estimated the standard error using an empirical function between standard deviation and mean track length given by Galbraith and Laslett (1997) (Fig. 4). They fitted the experimental data and standard errors of Yamada et al. (1995) with a function of two straight lines, one horizontal and the other with slope b_{SD}, joined by a smooth curve:

$$SD(L) = \exp\left\{2a_{SD} + 2b_{SD}\left[(\ln(L) - \ln 9) - \sqrt{(\ln(L) - \ln 9)^2 + c_{SD}}\right]\right\}. \tag{9}$$

When applied to the data set of $L_{>60}$ values from Yamada et al. (1995) and Tagami et al. (1998), we obtained the following best-fit parameters: $2a_{SE} = -0.44$, $2b_{SE} = -1.16$, $c_{SE} = 0.005$. These parameter values differ slightly from the values reported by Galbraith and Laslett (1997) due to the addition of the two

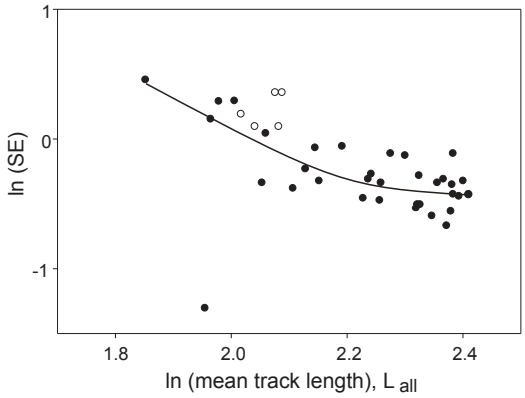

FIGURE 4. Empirically derived relationship between the mean track length and its standard deviation (SD), based on all annealing data from Tagami et al. (1998) (filled circles). For the proposed regression curve, the lowermost data point (in parentheses), which is based on only two measured track lengths, was neglected. Open circles show the standard error estimates that are visible in the figures of Kasuya and Naeser (1988).

new long-term annealing experiments. In Figure 4, those standard errors that are visible in the data plots of Kasuya and Naeser (1988) are shown for comparison[2], and indicate that the estimates of standard errors for Kasuya and Naeser (1988) were indeed in the same range as those for the Yamada et al. (1995) data.

A comparison of the weighting factors indicates that those derived from track-length data are generally higher than those determined from track-density data. The reason is the higher precision of track-length data compared to track-density data. Because the weighting is based on $SE(\gamma)$, all samples with a large difference between L and L_o are weighted much more strongly (Eq. 4). Accordingly, data from low-temperature and short-duration runs have a weaker influence on the regression analysis because L is only slightly smaller than L_0. The only track-density data that receive a stronger weighting than all track-length data are those with values lower than $L/L_0 = 0.25$. In this case, track-length measurements are few and very difficult to make resulting in large $SE(L)$ and $SE(\gamma)$. Track-density data, on the other hand, have errors in the 50% range (Carpéna 1992), but their calculated $SE(\gamma)$ is relatively small.

The best-fit results for zero-damage zircon are shown in Figure 5. In equation form, the parallel model is:

$$\gamma = 9.21 - 9976\left(\frac{1}{T}\right) + 0.222\ln(t) \quad (10)$$

with $R^2 = 0.988$ and $\chi^2_r = 1.99$, and the fanning model is

$$\gamma = -11.57 + 0.000276T\ln(t) + 0.011T \quad (11)$$

[2] The transformation of standard error SE(r), as indicated in the Kasuya and Naeser (1988) figures, into the standard deviation (SD), is done by:

$$SD = SE\sqrt{n}$$

where n = number of track length measurements. Kasuya and Naeser (1988) report that their minimum n was more than 30. Consequently, we have used a value of n = 31 for all their data.

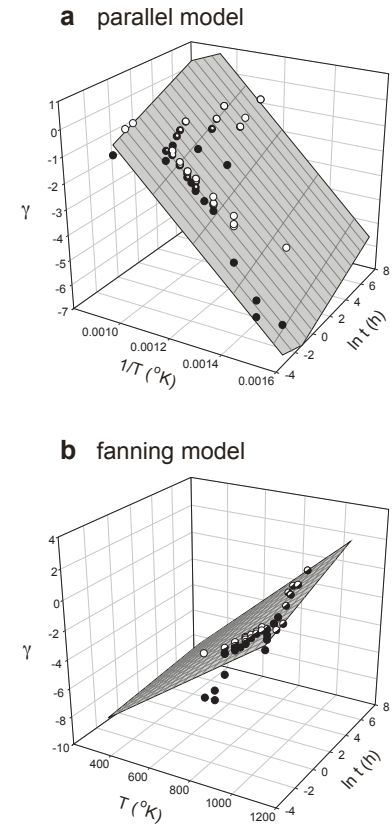

FIGURE 5. Best-fit solutions for zero-damage zircon fission track annealing experiments. The parallel model **(a)** predicts a flat plane in a γ-$1/T$-$\ln(t)$ space, whereas the fanning model **(b)** plane has a slight curvature in a γ-T-$\ln(t)$ space. For the fanning model, the offset of several points below the plane is visible. These points all have very small differences between L and L_0, thus, their $SE(\gamma)$ becomes very large, and their regression weighting factor is low.

with $R^2 = 0.992$ and $\chi^2_r = 1.34$ (Table 1). The regression calculation used 54 data points to estimate three parameters. The reduced χ^2_r is between 1 and 2, which means that the residuals are only slightly larger than the estimated uncertainties $SE(\gamma)$. In agreement with previous studies, the fanning model turns out to be slightly more consistent with the experimental data. Note that the combined data provide excellent fits despite the fact that the zero-damage data come from three different labs. However, it has to be kept in mind that the accuracy of these fits is in part due to the facts that (1) the Kasuya and Naeser (1988) and Yamada et al. (1995) data sets on one hand and the Carpéna (1992) data set on the other have a restricted overlap with respect to annealing experiment duration (Fig. 2), and (2) the applied weighting of the data according to their measurement uncertainties produces another bias of the importance of the data sets with respect to L/L_0.

DISCUSSION

Comparison with previous annealing models

For comparison we have used the same procedure as Tagami et al. (1998) to analyze annealing data for low damaged zircon

TABLE 1. Regression data of the different calculated models on fission track annealing

Data set	Data sources	n	Parallel model (Eq. 2)					Fanning model (Eq. 3)				
			a_p (±1σ)	b_p (±1σ)	c_p (±1σ)	R^2 (±1σ)	χ^2_r‡ (±1σ)	a_f (±1σ)	b_f (±1σ)	c_f (±1σ)	R^2 (±1σ)	χ^2_r‡ (±1σ)
Zero-damage zircon (zr)	Kasuya & Naeser 1988, Yamada et al. 1995, Carpena 1992	54	9.207 (0.130)	-9976 (127)	0.2216 (0.0172)	0.988	1.99	−11..57 (0.14)	2.755E-4 (0.189E-4)	1.075E-2 (0.014E-2)	0.992	1.34
Low-damage zr	Tagami et al. 1998	27	6.532 (0.215)	−7248 (192)	0.2039 (0.0063)	0.955	2.80	−10.77 (0.24)	2.599E-4 (0.078E-4)	1.026E-2 (0.027E-2)	0.966	2.14
Low- to moderate-damage zr	Kasuya & Naeser 1988, Tagami et al. 1990, Tagami et al. 1998	66	6.581 (0.050)	−7101 (39)	0.1736 (0.0029)	0.927	41.85	−11.41 (0.05)	2.472E-4 (0.037E-4)	1.125E-2 (0.006E-2)	0.915	48.59
Mixed-damage zr	Kasuya & Naeser 1988, Carpena 1992, Tagami et al. 1990, Tagami et al. 1998	120	6.221 (0.029)	−6855 (25)	0.1729 (0.0028)	0.951	33.29	−9..911 (0.031)	2.488E-4 (0.034E-4)	9.267E-3 (0.034E-3)	0.938	42.50

Notes: n = number of data, not included are the measurements at ambient temperatures. χ^2_r = reduced chi-square, χ^2_r = sum (residuals^2)/n−3, where 3 corresponds to the number of fit parameters.

samples (n = 27). The parallel model gives:

$$\gamma = 6.53 - 7248\left(\frac{1}{T}\right) + 0.204\ln(t) \quad (12)$$

with $R^2 = 0.955$ and $\chi^2_r = 2.80$. The fanning model gives:

$$\gamma = -10.77 + 0.000260T\ln(t) + 0.010T \quad (13)$$

with $R^2 = 0.966$ and $\chi^2_r = 2.14$. If we include other annealing experiments on damaged zircon, such as those of Kasuya and Naeser (1988) or Tagami et al. (1990), regression coefficients and reduced χ^2_r values become worse (Table 1). Different levels of α damage and annealing behavior deteriorate the statistics of the model fit and, interestingly, lead to relatively lower χ^2 values for the parallel model (Table 1). We conclude that the increase in density variation of α damage runs parallel to an increase in annealing behavior variation. Such variation in α damage density is common in natural zircon samples: even with a unimodal age distribution, single grains have different densities of α damage due to differences in U content and are therefore expected to show differences in their annealing behavior and closure temperature.

In Figure 6, the fanning iso-annealing contours for the zero-damage zircon model are compared to the Galbraith and Laslett (1997) fit for the Yamada et al. (1995) data, and the Tagami et al. (1998) model (thick lines). Both models refer to "low-damage" zircon samples, as these zircon samples had initial spontaneous track densities of around 4×10^6/cm^2 (Tagami et al. 1995b). Comparison of the models derived from zircon samples of different damage level is accomplished on the basis of the relative positions of their lower (i.e., low-temperature) and upper (i.e., high-temperature) PAZ boundaries. These boundaries are here defined by a 10 and 90% track-density reduction, respectively, as previously used by Durrani and Khan (1970) and Tagami and Dumitru (1996). The zero-damage model predicts the highest PAZ boundary temperatures, whereas Galbraith and Laslett (1997) are on the lower end. Fission tracks in zero-damage zircon samples seem to be most resistant to annealing.

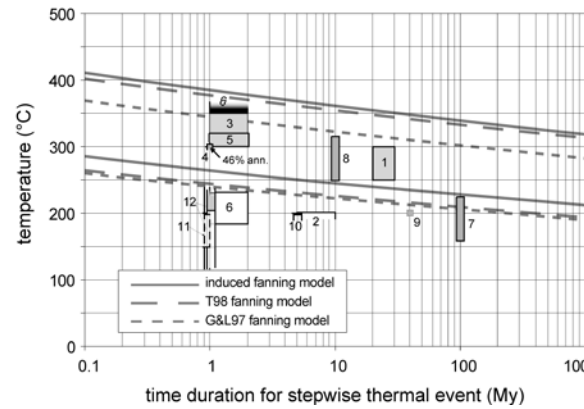

FIGURE 6. Comparison of three different zircon FT fanning annealing and geologic constraints on the zircon PAZ from the literature: solid thick lines = zero-damage model (this study); long-dashed thick lines = Tagami et al. (1998); short-dashed thick lines = Galbraith and Laslett (1997) model. The model PAZ boundaries were calculated as 10 and 90% track-density reduction lines based on the track length-density relationship of Tagami et al. (1990). Literature data: (1) Árkai et al. (1995), (2) Tagami et al. (1995a), (3) Carpéna and Caby (1984, gray area), (4) Ito and Tanaka (1995), (5) Rahn and Brandon (1998, area surrounded by dashed line), (6) Rahn et al. (2000), (7) Zaun and Wagner (1985), (8) Hasebe et al. (1997), (9) Ohmori et al. (1997), (10) Tagami and Shimada (1996), (11) Roden et al. (1993), (12) Hasebe et al. (2003). White boxes indicate conditions below the zircon FT PAZ, gray boxes conditions within the zircon FT PAZ, and one black box indicates totally reset zircon samples. Box boundaries are given as thick lines only where conditions are explicitly stated in the literature.

Geologic constraints on the zircon PAZ

Field constraints on the zircon PAZ can be divided into three groups according whether the zircon samples in the investigated rocks do not show any sign of partial annealing at a specific temperature (e.g., Tagami et al. 1995a; Tagami and Shimada 1996), they entered the PAZ without reaching its upper end (e.g., Carpéna and Caby 1984; Brandon and Vance 1992; Ito and Tanaka 1995; Wagner et al. 1997; Brandon et al. 1998; Rahn et al. 2000; Hasebe et al. 2003) or they reached complete annealing (e.g., Rahn et al. 2000). Zircon samples that enter the FT PAZ at its lower-temperature boundary will undergo track annealing at a rate that depends on the accumulated α-damage density. In sedimentary samples, fission tracks in zircon samples of different age and U content will have different annealing rates,

and while some young or U-poor zircon samples still retain their provenance age at a certain temperature, old or U-rich grains start annealing their fission tracks at the same conditions. In the high-*T* range of the PAZ, a well-defined component of completely reset zircon samples may occur with a component of only partially annealed grains. The advantage of this behavior is obvious: the presence of high-damage zircon samples allows that fraction to reset well before the last grains are totally reset and therefore record geologically meaningful information (see e.g., Brandon et al. 1998; Graver et al. 2002).

Several studies have proposed that lower-greenschist or blueschist facies conditions (i.e., temperatures up to 350 °C) are needed for complete track annealing in detrital zircon samples (Carpéna and Caby 1984; Rahn and Brandon 1998; Rahn et al. 2000). In the Central Alps, which are known for their moderate to fast Neogene cooling rates (Hurford 1986; Hunziker et al. 1992), partially reset zircon samples exist up to maximum metamorphic temperatures of >300 °C (Rahn et al. 2000) as constrained by fluid inclusion, vitrinite reflectance, and mineral paragenesis data. Brandon et al. (1998) reported zircon grain age distributions from the Olympic subduction complex, Washington State, with components of completely reset and only partially reset ages. For the corresponding localities, metamorphic assemblages show pumpellyite-actinolite facies and geothermometers suggest maximum temperatures of ~320 °C (Rahn and Brandon 1998). Ito and Tanaka (1995) reported zircon FT ages from a borehole with a bottom-hole temperature of 295 °C where the zircon samples underwent only 46% track-length reduction during a ~1 myr heating event. For a deep bore hole close to Vienna, Austria, Tagami et al. (1995a) observed no traces of annealing, even though measured bottom temperatures of 200 °C seem to have persisted over the last 5–10 myr. In a similar study on two boreholes from Japan, Hasebe et al. (2003) observed a decrease of mean track length for samples with a present borehole temperature above 205 °C. The thermal conditions were estimated to have persisted for a duration of 1 myr.

A study of Carpéna and Caby (1984) presented unreset zircon ages from the Western Alps ophiolites, which contain Alpine metamorphic minerals such as lawsonite, glaucophane, and jadeite. The authors estimated metamorphic conditions of 0.6–0.8 GPa and 300–350 °C for this paragenesis. From the late Triassic-early Jurassic zircon ages, we would assume that these zircon samples would have accumulated a large density of α damage and would therefore reset at rather low temperatures. With one exception, however, all zircon samples show an unusually low track density. In this case, not the age, but the low U content most probably has caused a low α-damage density and a high resistance to FT annealing.

The available geologic evidence for zircon PAZ boundaries from the literature is compiled in a log time vs. temperature diagram (Fig. 6). All sources provide detailed information about the state of zircon annealing, and independent information about the duration of track accumulation before, and the maximum temperature and duration of the undergone heating event. Not included are constraints from the ultra-deep borehole at the Kola Peninsula (see Tagami et al. 1998), because for these data, the thermal setting has only been estimated, mainly by assuming a constant temperature (T = 212 °C, measured at the bottom after drilling) for the last ~250 myr. The same insufficiently detailed thermal and temporal information is provided for the KTB bore hole, leading to a rejection of these data for the here presented compilation.

The temperature and time information of most of the compiled geologic examples scatters along a zone that is oblique to the modeled PAZ boundaries. The examples plot within the PAZ boundaries for short-duration heating events, but below the PAZ (or its lower boundary) for long-duration heating episodes. Long-duration changes in thermal conditions imply that zircon samples with high α damage are involved in annealing, leading to the strongest deviation from the predictions of a zero-damage annealing model. In contrast, fast changes in thermal conditions are, in general, compatible with low α-damage accumulation rates in zircon and, in this case, zircon samples behave more according to the predictions of low damage annealing models. One interesting outlier to this general trend comes from a study with very old partially reset zircon samples that underwent a short-term heating event (<1 myr, Roden et al. 1993). Independent estimates based on fluid inclusion data and conodont alteration color suggest temperatures <200 °C. Other temperature indicators suggest a maximum temperature within a range of 100–200 °C (Roden et al. 1993). Accordingly, zircon samples in Roden et al. (1993) start to anneal their accumulated fission tracks below 200 °C, which is much earlier, as e.g., demonstrated by Rahn et al. (2000) for Alpine zircon samples that show no evidence of annealing in the temperature range of 180–230 °C (determined by fluid inclusion homogenization temperatures). Recent studies have found similar situations where the annealing of a small fraction of radiation damaged grains occurred at temperatures that were probably 200 °C or less (Garver et al. 2002). These studies illustrate that the α-damage density of the zircon samples, which was accumulated according to their detrital age, determines the annealing behavior of the FTs.

Geologic evidence for the zircon FT closure temperature

The closure temperature, T_c, of the zircon FT system was estimated in a large number of geochronologic field studies, where the investigated rocks underwent monotonic cooling from temperatures above the zircon PAZ to temperatures below it (e.g., Harrison et al. 1979; Zeitler 1985; Hurford 1986; Fitzgerald and Gleadow 1988; Gebauer et al. 1997; Brandon et al. 1998; Scott et al. 1998; Batt et al. 1999). Studies with fast cooling rates are of particular interest, as they might represent a situation where zircon samples move through the PAZ in a nearly damage-free state. In this case, the FT system should most closely follow our results for zero-damage zircon samples. In a study on the very fast exhumation of the ultra-high pressure rocks of the Dora Maira, Western Alps, Gebauer et al. (1997) used a T_c of 290 ± 40 °C in accordance with Tagami and Shimada (1996) and Wagner et al. (1997). On this basis, cooling rates of to 80 °C per myr were estimated to have occurred subsequent to deepest burial. The FT T_c predicted from the zero-damage annealing model is 338 °C, whereas the Galbraith and Laslett (1997) and Tagami et al. (1998) model predicts T_c = 306 and 312 °C, respectively (Fig. 7). In the Gebauer et al. (1997) study, the closure temperature of zircon was taken from the literature, and not constrained by geologic evidence.

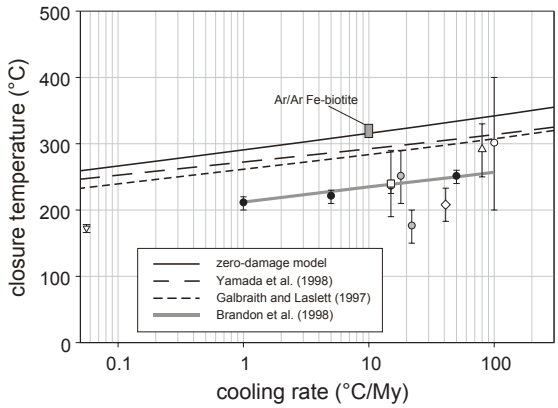

FIGURE 7. Predicted closure temperatures for the case of constant cooling of zircon samples across the PAZ from the zero-damage (solid line), and two low-damage models (Tagami et al. 1998, long dashed line), and (Galbraith and Laslett 1997, short dashed line). The predictions are compared to geologic constraints from the literature: gray line = Brandon et al. (1998); circles = constraints based on a direct comparison between Ar/Ar age spectra of K-feldspar [black = Scott et al. (1998), gray = Batt et al. (1999), white = Hoisch et al. (1997)]; open diamond = Harrison et al. (1979), recalculated according to Brandon et al. (1998); open square = Hurford (1986); triangle = Gebauer et al. (1997); and upside-down triangle = Koul et al. (1988). For comparison, the temperature range for closure of the Ar/Ar system in Fe-rich biotite at a cooling rate of 10 °C/myr from Grove and Harrison (1996) is indicated and coincides with the closure conditions of the zero-damage zircon FT model.

Several studies determined the zircon FT closure temperature based on other geochronologic systems with neighboring closure temperatures. In those cases, the applied closure temperatures of these neighboring systems had a strong effect on the determination of the zircon closure temperature. Commonly, such neighboring geochronologic systems are the apatite FT system and the K-Ar and Rb-Sr systems of biotite and muscovite, which are also dependent on cooling rates or the duration of a heating event (e.g., Grove and Harrison 1996; Ketcham et al. 1999). Furthermore, the Ar- and Sr-isotopic systems in biotite and muscovite may have higher closure temperatures than previously assumed in cases of moderate to fast cooling rates, based on comparisons with stable isotope and other thermometric data (Kirschner et al. 1996). In a geothermal field with a short-duration thermal pulse, Del Moro et al. (1982) and Villa and Puxeddu (1994) presented evidence for closing of the K-Ar and Rb-Sr systems in biotite at >400 °C. Estimates of the zircon closure temperature based on other isotopic systems are limited to the understanding of closure in those systems.

The only other geochronologic method that allows direct link of ages with similar temperatures is the Ar/Ar K-feldspar system. We have computed available studies with a combination of Ar/Ar K-feldspar and zircon FT ages. Previous studies without the step-heating procedure showed varying relationships between Ar/Ar K-feldspar and zircon FT ages (e.g., Harrison et al. 1979; Zeitler 1985; Shibata et al. 1990). Step heating was, however, used by Hoisch et al. (1997), Scott et al. (1998), and Batt et al. (1999). With the help of the Ar/Ar K-feldspar step-heating ages and the thermal history derived thereof, the closure temperature of the zircon system can be bracketed by the envelope of the modeled K-feldspar time-temperature path. By this procedure, Hoisch et al. (1997) estimated a zircon T_c of ~300 °C for a rapid cooling rate of 100 °C/Ma. Because the envelope of their K-feldspar model turned out to have a very steep time-temperature slope in the range of the zircon FT age, this estimate has a considerable uncertainty.

Our compilation of literature data is shown in Figure 7, and compared to the calculated relations between closure temperature and cooling rate (Galbraith and Laslett 1997; Tagami et al. 1998; this study). We used the method of Dodson (1979) to estimate effective closure temperatures from laboratory annealing data. The zero-damage model closure temperature plots approximately 25–30 °C above the Galbraith and Laslett (1997) curve. It is interesting to note that the zero-damage model predictions are in the range of closure of the Ar/Ar system derived from diffusion experiments on Fe-rich biotites (Grove and Harrison 1996).

Most zircon FT closure temperatures derived from geologic data scatter at distinctly lower values than estimated from the two zircon annealing models, and lie close to the published curve of Brandon et al. (1998). In particular for high cooling rates, however, the field data tend to shift toward the values predicted by the low-damage model of Galbraith and Laslett (1997) and Tagami et al. (1998), and might, with even faster cooling rates, approach the predictions of the zero-damage model. The latter predicts that, in this case, zircon FT closure would be in the temperature range of the closure of the biotite Ar/Ar system.

The applicability of the zero-damage model in the field

From our compilation it is evident that there is no direct geologic evidence for the zero-damage model, but observations are consistent with an increase of annealing temperatures with decreasing damage density. For both data sets (Figs. 6 and 7), geologic constraints for zircon FT annealing are oblique to established model predictions, and consistently move to the high-temperature side for short-duration events. In both cases, the predictions by Galbraith and Laslett (1997) and Tagami et al. (1998) for low-damage zircon samples estimate high temperatures, and only seem to agree with field constraints for short-duration temperature changes. In both cases, the applicability of the zero-damage annealing model seems to be limited to cases of very fast cooling or very short thermal pulses.

Rather than being directly applicable to geologic settings, the zero-damage model provides an upper boundary for the annealing rate of fission tracks in zircon. Its applicability presumably is restricted to the following cases: (1) In settings of very fast cooling from very high temperatures, the zero-damage annealing model predicts a correct zircon closure temperature, when practically no α damage is accumulated before the onset of FT retention. (2) In settings where mixed components of a zircon population undergo partial to total resetting, the zero-damage annealing model should predict maximum temperature conditions for total annealing, and thus can be used as a thermometer and mappable isotherm, especially if sediments include a very young (e.g., volcanic) or low-U component.

The temperature difference between the low- and the zero-damage models (Fig. 6) is less than 50 °C for the PAZ boundaries. A clear distinction between the different proposed models based

on geologic evidence requires a high precision of the temperature estimate during a thermal pulse or metamorphic event. Most temperature-sensitive parameters used to quantify very low- to low-grade metamorphism, such as vitrinite reflectance, mineral paragenesis, chlorite, and stable isotope thermometers, rarely provide a precision better than ±20 °C. Therefore, it might be difficult to distinguish between these different annealing models on the basis of such data. However, given the fact that the fanning and parallel relationships differ in their long-duration predictions (at 1 to 100 myr) by up to 100 °C (Fig. 1), future emphasis should be put on the distinction between these two existing relationships on the basis of geologic field evidences.

The influence of α-damage on FT annealing

Based on the proposed zero-damage model, the influence of α damage on the annealing properties can be evaluated qualitatively. For this purpose, we consider the ratio $\gamma_{obs}/\gamma_{pred}$, corresponding to the γ as observed in the annealing data and γ as predicted by the zero-damage model. If α-damage is increasing the rate of FT annealing in zircon, we expect the γ ratio to show values below 1 for α-decay-damaged zircon samples. Ratios are calculated for all annealing data from Tagami et al. (1998) and Kasuya and Naeser (1988), and are presented in Figure 8, plotted vs. the initial track densities observed in the zircon samples prior to the annealing experiment. The track densities here serve as a proxy for radiation damage density. Assuming that the α-damage PAZ is situated at higher temperatures relative to the FT PAZ, as suggested from experimental annealing temperatures (Geisler 2002), the initial α-damage density in a zircon grain is not expected to change significantly during any annealing experiment that stops before total FT annealing. In addition to the data of Kasuya and Naeser (1988), Tagami et al. (1990), and Yamada et al. (1995), we have also added the Zaun and Wagner (1985) data to the compilation (Fig. 6). The Zaun and Wagner (1985) data are poorly constrained with respect to their published track density range, but in comparison with the other data, show the strongest difference from the zero-damage model, and the highest track densities.

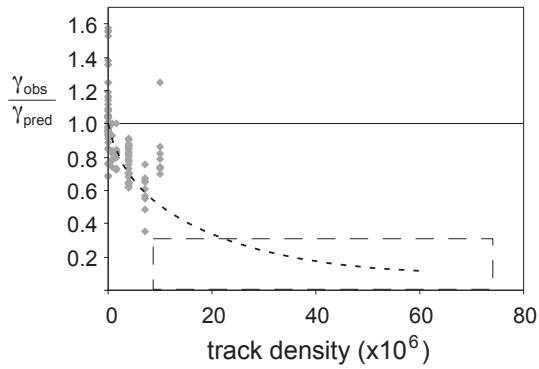

FIGURE 8. Compilation of zero-damage zircon FT (track density = 0), and natural zircon FT experiments (Kasuya and Naeser 1988; Tagami et al. 1990; Tagami et al. 1998) and their difference from the predictions of a zero-damage model. A $\gamma_{obs}/\gamma_{pred}$ value of 1 (horizontal line) indicates agreement with the zero-damage model. The data of Zaun and Wagner (1985) are indicated by a dashed-lined box representing their varying offset from the zero-damage model and their large variation in reported track densities (recalculated to the initial track density before annealing). The curved trend shows the predicted influence of α damage (estimated by the initial track density) on zircon FT annealing.

The plotted data (Fig. 8) show a trend that quickly moves away from the line of equity with increasing track density, but seems to behave asymptotically toward a maximum deviation from the predictions in an α-damage-free zircon at high track density. The relationship between annealing rate and α-damage density (ρ_α) can be estimated qualitatively from existing data on natural zircon samples and a zero-damage zircon annealing model proposed here. A plausible empirical function for these data is

$$\gamma = a_f + b_f T \ln(t) + c_f T + d_f \ln(\rho_\alpha) \quad (14)$$

Such an equation has the advantage of providing a linear relationship between γ and the fit parameters *a*-*d*. Alternatively, an equation is proposed where the parameter *b* is interpreted in terms of the activation energy of the annealing process (Märk et al. 1981; Modgil and Virk 1985; Sandhu et al. 1990; Virk 1995) and changes as a function of ρ_α. In this case, Equation 3 is modified to:

$$\gamma = a_f + b_f(\rho_\alpha) T \ln(t) + c_f T \quad (15)$$

or

$$\gamma = a_f + b_f(\rho_\alpha)[T \ln(t) + c_f T] \quad (16)$$

depending on whether we refer to a fanning model with fixed fanning point or with a fanning point drifting along the $1/T = 0$ axis (Yamada et al. 1995; Ketcham et al. 1999). Because:

$$\rho_\alpha = \rho_\alpha(t, T) \quad (17)$$

where *t* accounts for both the accumulation of α-damage and the time effect in annealing, a general conclusion is that iso-annealing curves in an Arrhenius plot cannot be parallel, and the assignment of the *b* parameter to an activation energy, which is dependent on a second annealing process, would also give a physical explanation on why the fanning relationship should give a better statistical fit to the data.

For the establishment of an α damage integrating model, as preliminarily outlined by Equations 14–16, much more experimental annealing data, in particular for the annealing of fission tracks under high α-damage-density conditions, are needed. Because there is evidence of a marked overlap of the α PAZ and the FT PAZ, the establishment of such an α-damage-integrating model will have to consider the thermal and temporal brackets of α-damage annealing.

CONCLUDING REMARKS

Despite restricted use for geologic applications, the proposed zero-damage FT annealing model has important implications for understanding FT annealing in zircon samples. The available data for zero-damage zircon samples (Fig. 2a) show a remarkable consistency that cannot be found in any other comparison

among the various zircon annealing experiments. Annealing experiments with zero-damage zircon samples are proposed as the basis for further experimental investigations. As a next step, suitable zircon samples have to be found that show the smallest possible grain to grain variation in α-damage density, i.e., preferably have the same age and U content (and average Th/U ratio, see Garver and Kamp 2002). As a counterpart to existing annealing data, experiments on FT annealing in very high-damage zircon samples are particularly important. Furthermore, the time-temperature relationship between FT annealing and α-damage annealing has to be evaluated in more detail, e.g., by combined annealing experiments. One important step in this direction was the establishment of α-damage density quantification by Raman spectroscopy (Nasdala et al. 1995, 2001).

A compilation of geologic constraints on FT annealing in zircon samples reveals that none of the existing zircon FT annealing models is able to explain the range of available field evidence. Temperature conditions predicted from the zero-damage model are thought to represent an upper temperature limit for zircon FT annealing. Rather than assuming a fixed closure temperature for the zircon FT system, we have to apply a value that is dependent not only on the cooling rate but also on the U and Th content, because the annealing behavior of fission tracks in zircon samples is sensitive to α damage, in particular in the very low α-damage density range (Fig. 8).

As an upper temperature limit for zircon annealing, the zero-damage model might represent a mappable isotherm in areas of sub-greenschist to low-greenschist facies metamorphism. Because the temperatures for total resetting the FT system depend not only on the annealing duration, but also on the amount of accumulated α-damage, this thermometer is also dependent on the U content and thermal history of the zircon samples involved. In the case of no further constraints, the zero-damage model may provide a maximum temperature value.

ACKNOWLEDGMENTS

This study was performed while M.R. was a visiting scholar at Yale University, supported by Swiss National Science Foundation grant no. 8220-050380. We thank R. Fleischer, M. Kasuya, C. Naeser, and T. Tagami for their help in getting original data out of old papers, and T. Geisler for introduction into the physical meaning of α damage in the zircon crystal lattice. Four anonymous reviewers, R. Ewing and R. Ketcham helped by their suggestions to markedly improve the quality of the manuscript.

REFERENCES CITED

Amin, Y.M. (1988) Effect of damage on the etching and X-ray diffraction properties of zircon. Nuclear Tracks and Radiation Measurements, 15, 119–123.

Árkai, P., Balogh, K., and Dunkl, I. (1995) Timing of low-temperature metamorphism and cooling of the Paleozoic and Mesozoic formations of the Bükkium, innermost Western Carpathians, Hungary. Geologische Rundschau, 84, 334–344.

Batt, G.E., Kohn, B.P., Braun, J., McDougall, I., and Ireland, T.R. (1999) New Insight into the dynamic development of the Southern Alps, New Zealand, from detailed thermochronological investigation of the Mataketake Range pegmatites. In Ring, U., Brandon, M.T., Lister, G.S., and Willett, S.D., Eds., Exhumation processes; normal faulting, ductile flow and erosion, p. 261–282. Geological Society of London Special Publications, 154.

Brandon, M.T. and Vance, J.A. (1992) Tectonic evolution of the Cenozoic Olympic subduction complex, Washington State, as deduced from fission track ages for detrital zircons. American Journal of Science, 292, 565–636.

Brandon, M.T., Roden-Tice, M.K., and Garver, J.I. (1998) Late Cenozoic exhumation of the Cascadia accretionary wedge in the Olympic Mountains, NW Washington State. Geological Society of America Bulletin, 110, 985–1009.

Capitani, G.C., Leroux, H., Doukhan, J.C., Ríos, S., Zhang, M., and Salje, E.K.H. (2000) A TEM investigation of natural metamict zircons: structure and recovery of amorphous domains. Physics and Chemistry of Minerals, 27, 545–556.

Carlson, W.D., Donelick, R.A., and Ketcham, R.A. (1999) Variability of apatite fission-track annealing kinetics I: Experimental results. American Mineralogist, 84, 1213–1223.

Carpéna, J. (1992) Fission track dating of zircon: zircons from Mont Blanc Granite (French-Italian Alps). The Journal of Geology, 100, 411–421.

Carpéna, J. and Caby, R. (1984) Fission-track evidence for late Triassic oceanic crust in the French Occidental Alps. Geology, 12, 108–111.

Chakoumakos, B.C., Murakami, T., Lumpkin, G.R., and Ewing, R.C. (1987) Alpha-decay-induced fracturing in zircon: the transition from the crystalline to the metamict state. Science, 236, 1556–1559.

Crowley, K.D, Cameron, M., and Schaefer, R.L. (1991) Experimental studies of annealing of etched fission tracks in fluorapatite. Geochimica et Cosmochimica Acta, 55, 1449–1465.

Del Moro, A., Puxeddu, M., Radicati di Brozolo, F., and Villa, I.M. (1982) Rb-Sr and K-Ar ages on minerals at temperatures of 300–400 °C from deep wells in the Larderello geothermal field (Italy). Contributions to Mineralogy and Petrology, 81, 340–349.

Dodson, M.E. (1979) Theory of cooling ages. In E. Jaeger and J.C. Hunziker, Eds., Lectures in isotope geology, p. 194–202. Springer-Verlag.

Durrani, S.A. and Khan, H.A. (1970) Annealing of fission tracks in tektites: corrected ages of bediasites. Earth and Planetary Science Letters, 9, 431–445.

Ewing, R.C. (1994) The metamict state: 1993–the centennial. Nuclear Instruments and Methods of Physical Research, B91, 22–29.

Farnan, I. and Salje, E.K.H. (2001) The degree and nature of radiation damage in zircon observed by ^{29}Si nuclear magnetic resonance. Journal of Applied Physics, 89, 2084–2090.

Fitzgerald, P.G. and Gleadow, A.J.W. (1988) Fission-track geochronology, tectonics and structure of the Transantarctic Mountains in northern Victoria Land, Antarctica. Chemical Geology, 73, 169–198.

Fleischer, R.L., Price, P.B., and Walker, R.M. (1964) Fission track ages of zircon. Journal of Geophysical Research, B69, 4885–4888.

Fleischer, R.L., Price, P.B., and Walker, R.M. (1965) Effects of temperature, pressure, and ionization of the formation and stability of fission tracks in minerals and glasses. Journal of Geophysical Research, B70, 1497–1502.

Galbraith, R.F. and Laslett, G.M. (1997) Statistical modelling of thermal annealing of fission tracks in zircon. Chemical Geology, 140, 123–135.

Gallagher, K. (1995) Evolving temperature histories from apatite fission-track data. Earth and Planetary Science Letters, 136, 421–435.

Garver, J.I. and Brandon, M.T. (1994) Erosional denudation of the British Columbia Coast Ranges as determined from fission-track ages of detrital zircon from the Tofino Basin, Olympic Peninsula, Washington. Geological Society of America Bulletin, 106, 1398–1412.

Garver, J.I. and Kamp, P.J.J. (2002) Integration of zircon color and zircon fission-track zonation patterns in orogenic belts: application to the Southern Alps, New Zealand. Tectonophysics, 349, 203–219.

Garver, J.I., Brandon, M.T., Roden-Tice, M.K., and Kamp, P.J.J. (1999) Exhumation history of orogenic highlands determined in detrital fission track thermochronology. In Ring, U., Brandon, M.T., Lister, G.S., and Willett, S.D., Eds., Exhumation processes; normal faulting, ductile flow and erosion, p. 283–304. Geological Society of London Special Publications, 154.

Garver, J.I., Riley, B.C.D., and Wang, G. (2002) Partial resetting of fission tracks in detrital zircon. Geotemas, 4, 73–75.

Gebauer, D., Schertl, H.-P., Brix, M., and Schreyer, W. (1997) 35 Ma old ultrahigh-pressure metamorphism and evidence for very rapid exhumation in the Dora Maira Massif, Western Alps. Lithos, 41, 5–24.

Geisler, T. (2002) Isothermal annealing of partially metamict zircon: evidence for a three-stage recovery process. Physics and Chemistry of Minerals, 29, 420–429.

Grove, M. and Harrison, T.M. (1996) ^{40}Ar* diffusion in Fe-rich biotite. American Mineralogist, 81, 940–951.

Harrison, T.M., Armstrong, R.E., Naeser, C.W., and Harakal, J. E. (1979) Geochronology and thermal history of the Coast Plutonic complex, near Prince Rupert, British Columbia. Canadian Journal of Earth Sciences, 16, 400–410.

Hasebe, N., Tagami, T., and Nishimura, S. (1993) Evolution of the Shimanto accretionary complex: a fission-track thermichronological study. In Underwood, M.B., Ed., Thermal Evolution of the Tertiary Shimanto Belt, Southwest Japan: An Example of Ridge-Trench Interaction, p. 121–136. Geological Society of London Special Paper, 273.

Hasebe, N., Tagami, T., and Nishimura, S. (1997) Melange-forming processes in the development of an accretionary prism: Evidence from fission track thermochronology. Journal of Geophysical Research, 102, 7659–7672.

Hasebe, N., Mori, S., Tagami, T., and Matsui, R. (2003) Geological partial annealing zone of zircon fission-track system: additional constrains from the deep drilling MITI-Nishikubiki and MITI-Mishima. Chemical Geology, 199, 45–52.

Hoisch, T.D., Heizler, M.T., and Zartman, R.E. (1997) Timing of detachment faulting in the Bullfrog Hills and Bare Mountain area, southwest Nevada: Inferences from ^{40}Ar/^{39}Ar, K-Ar, U-Pb, and fission track thermochronology. Journal of Geophysical Research, B102, 2815–2833.

Holland, H.D. and Gottfried, D. (1955) The effect of nuclear radiation on the structure of zircon. Acta Crystallographica, 8, 291–300.

Hunziker, J.C., Desmons, J., and Hurford, A.J. (1992) Thirty-two years of geochronological work in the Central and Western Alps: a review on seven maps, 59p. Mémoires de Geologie (Lausanne), 13.

Hurford, A.J. (1986) Cooling and uplift patterns in the Lepontine Alps, South Central Switzerland, and an age of vertical movement on the Insubric fault line. Contributions to Mineralogy and Petrology, 92, 413–427.

Ito, H. and Tanaka, K. (1995) Insights on the thermal history of the Valles Caldera, New Mexico: evidence from zircon fission-track analysis. Journal of Volcanology and Geothermal Research, 67, 153–160.

Kasuya, M. and Naeser, C.W. (1988) The effect of α-damage of fission-track annealing in zircon. Nuclear Tracks and Radiation Measurements, 14, 477–480.

Ketcham, R.A., Donelick, R.A., and Carlson, W.D. (1999) Variability of apatite fission-track annealing kinetics: 3. Extrapolation to geologic time scales. American Mineralogist, 84, 1235–1255.

Kirschner, D.L., Hunziker, J.C., and Cosca, M. (1996) Closure temperature of argon in micas; a review and reevaluation based on Alpine samples. Abstracts with Programs, Geological Society of America, 28, 441.

Koshimizu, S. (1993) Comparison of thermal stability between internal and external surfaces of zircon. Nuclear Tracks and Radiation Measurements, 22, 785–788.

Koul, S.L., Wilde, A.R., and Tickoo, A.K. (1988) A thermal history of the Proterozoic East Alligator River Terrain, N. T., Australia: a fission track study. Tectonophysics, 145, 101–111.

Krishnaswami, S., Lal, D., Prabhu, N., and MacDougall, D. (1974) Characteristics of fission tracks in zircon: Applications to geochronology and cosmology. Earth and Planetary Science Letters, 22, 51–59.

Larsen, E.S., Keevil, N.B., and Harrison, H.C. (1952) Method for determining the age of igneous rocks using the accessory minerals. Geological Society of America Bulletin, 63, 1045–1052.

Laslett, G.M. and Galbraith, R.F. (1996) Statistical modelling of thermal annealing of fission tracks in apatite. Geochimica et Cosmochimica Acta, 60, 5117–5131.

Laslett, G.M., Green, P.F., Duddy, I.R., and Gleadow, A.J.W. (1987) Thermal annealing of fission tracks in apatite, 2: A quantitative analysis. Chemical Geology, 65, 1–13.

Märk, T.D., Pahl, M., and Vartanian, R. (1981) Fission track annealing and fission track age-temperatrue relationship in sphene. Nuclear Technology, 52, 295–305.

Modgil, S.K. and Virk, H.S. (1985) Annealing of fission fragment tracks in inorganic solids. Nuclear Instruments and Methods in Physics Research, B12, 212–218.

Murakami, T., Chakoumakos, B.C., Ewing, R.C., Lumpkin, G.R., and Weber, W.J. (1991) Alpha-decay event damage in zircon. American Mineralogist, 76, 1510–1532.

Nasdala, L., Irmer, G., and Wolf, D. (1995) The degree of metamictisation in zircon: a Raman spectroscopy study. European Journal of Mineralogy, 7, 471–478.

Nasdala, L., Pidgeon, R.T., and Wolf, D. (1999) Heterogeneous metamictization of zircon on a microscale. Geochimica et Cosmochimica Acta, 60, 1091–1097.

Nasdala, L., Wenzel, M., Vavra, G., Irmer, G., Wenzel, T., and Kober, B. (2001) Metamictization of natural zircon; accumulation vs. thermal annealing of radioactivity-induced damage. Contributions to Mineralogy and Petrology, 141, 125–144.

Ohmori, K., Taira, A., Tokuyama, H., Sakaguchi, A., Okamura, M., and Aihara, A. (1997) Paleothermal structure of the Shimanto accretionary prism, Shikoku, Japan; role of an out-of sequence thrust. Geology, 25, 327–330.

Palenik, C.S., Nasdala, L., and Ewing, R.C. (2003) Radiation damage in zircon. American Mineralogist, 88, 770–781.

Press, W.H., Teukolsky, S.A., Vetterling, W.T., and Flannery, B.P. (1992) Numerical Recipes in Fortran: The Art of Scientific Computing, 963p. Cambridge University Press, Cambridge UK.

Pupin, J.P. (1980) Zircon and granite petrology. Contributions to Mineralogy and Petrology, 73, 207–220.

Rahn, M.K. and Brandon, M. T. (1998) Prograde subgreenschist metamorphism in the Olympic Mountains: constraints on mineral stability and partial annealing temperatures for zircon fission tracks. EOS Transactions, supplementary abstract volume, AGU Spring Meeting, Boston, S380.

Rahn, M.K., Mullis, J., Brandon, M.T., and Hurford, A.J. (2000) Field constraints on the zircon fission track partial annealing zone boundaries in fast evolving orogens. GSA Annual Meeting 2000, AAPG, A–152.

Ríos, S., Salje, E.K.H., Zhang, M., and Ewing, R.C. (2000) Amorphization in zircon: evidence for direct impact damage. Journal of the Physics of Condensed Matter, 12, 2401–2412.

Roden, M.K., Elliott, W.C., Aronson, J.L., and Miller, D.S. (1993) A comparison of fission-track ages of apatite and zircon to the K-Ar ages of illite-smectite (I/S) from Ordovician K-Bentonites, southern Appalachian Basin. The Journal of Geology, 101, 633–641.

Sandhu, A.S, Singh, L., Ramola, R.C., Singh, S., and Virk, H.S. (1990) Annealing kinetics of heavy ion radiation damage in crystalline minerals. Nuclear Instruments and Methods in Physics Research, B46, 122–124.

Scott, R.J., Foster, D.A., and Lister, G.S. (1998) Tectonic implications of rapid cooling of lower plate rocks from the Buckskin-Rawhide metamorphic core complex, west-central Arizona. Geological Society of America Bulletin, 110, 588–614.

Shibata, K., Danhara, T., and Takagi, H. (1990) Concordance between K-Ar ages of K-feldspar and fission-track ages of zircon in Cretaceous granitic rocks from Japan. Geochemical Journal, 24, 187–192.

Tagami, T. and Dumitru, T.A. (1996) Provenance and thermal history of the Franciscan accretionary complex; constraints from fission track thermochronology. Journal of Geophysical Research, B101, 11353–11364.

Tagami, T. and Shimada, C. (1996) Natural long-term annealing of the zircon fission track system around a granitic pluton. Journal of Geophysical Research, B101, 8245–8255.

Tagami, T., Ito, H., and Nishimura, S. (1990) Thermal annealing characteristics of spontaneous fission tracks in zircon. Chemical Geology, 80, 159–169.

Tagami, T., Hurford, A.J., and Carter, A. (1995a) Natural long-term annealing of the zircon fission-track system in Vienna Basin deep borehole samples; constraints upon the partial annealing zone and closure temperature. Chemical Geology, 130, 147–157.

Tagami, T., Uto, K., Matsuda, T., Hasebe, N., and Matsumoto, A. (1995b) K-Ar biotite and fission-track zircon ages of the Nisatai Dacite, Iwate Prefecture, Japan: A candidate for Tertiary age standard. Geochemical Journal, 29, 207–211.

Tagami, T., Galbraith, R.F., Yamada, R., and Laslett, G.M. (1998) Revised annealing kinetics of fission tracks in zircon and geological implications. In Van den haute, P. and De Corte, F., Eds., Advances in Fission-Track Geochronology, p. 99–112. Kluwer Academic Publishers, Netherlands.

Trachenko, K., Dove, M., and Salje, E.K.H. (2003) Large swelling and percolation in irradiated zircon. Journal of the Physics of Condensed Matter, 15, L1–L7.

Villa, I.M. and Puxeddu, M. (1994) Geochronology of the Larderello geothermal field: new data and the "closure temperature" issue. Contributions to Mineralogy and Petrology, 115, 415–426.

Virk, H.S. (1995) Single activation energy model of radiation damage in solid state nuclear track detectors. Radiation Effects and Defects in Solids, 133, 87–95.

Wagner, G.A., Coyle, D.A., Duyster, J., Henjes-Kunst, F., Peterek, A., Schröder, B., Stöckhert, B., Wemmer, K., Zulauf, G., Ahrendt, H., Bischoff, R., Hejl, E., Jacobs, J., Menzel, D., Nand Lal, Van den Haute, P., Vercoutere, C., and Welzel, B. (1997) Post-Variscan thermal and tectonic evolution of the KTB site and its surroundings. Journal of Geophysical Research, B102, 18221–18232.

Weber, W.J., Ewing, R.C., and Wang, L.-M. (1994) The radiation-induced crystalline-to-amorphous transition in zircon. Journal of Material Research, 9, 688–698.

Willett, S.D. (1997) Inverse modeling of annealing of fission tracks in apatite 1: A controlled random search method. American Journal of Science, 297, 939–969.

Yamada, R., Tagami, T., Nishimura, S., and Ito, H. (1995) Annealing kinetics of fission tracks in zircon: an experimental study. Chemical Geology, 122, 249–258.

Zaun, P.E. and Wagner, G.A. (1985) Fission track stability in zircons under geological conditions. Nuclear Tracks and Radiation Measurements, 10, 303–307.

Zeitler, P.K. (1985) Cooling history of the NW Himalaya, Pakistan. Tectonics, 4, 127–151.

Zhang, M. and Salje, E.K.H. (2001) Infrared spectroscopic analysis of zircon: Radiation damage and the metamict state. Journal of the Physics of Condensed Matter, 13, 3057–3071.

Zhang, M., Salje, E.K.H., Capitani, G.C., Leroux, H., Clark, A.M., Schlüter, J., and Ewing, R.C. (2000) Annealing of α-decay damage in zircon: a Raman spectroscopic study. Journal of the Physics of Condensed Matter, 12, 3131–3148.

MANUSCRIPT RECEIVED JANUARY 20, 2003
MANUSCRIPT ACCEPTED NOVEMBER 12, 2003
MANUSCRIPT HANDLED BY ROBERT DYMEK